THE JOURNAL OF BIOLOGICAL CHEMISTRY
Vol. 275, No. 4, Issue of January 28, pp. 2817–2824, 2000

Printed in U.S.A.

Mapping the Inter-RNA Interaction of Bacterial Virus Phi29 Packaging RNA by Site-specific Photoaffinity Cross-linking*

(Received for publication, June 1, 1999, and in revised form, October 5, 1999)

Kyle Garver and Peixuan Guo‡

From the Department of Pathobiology, Purdue University, West Lafayette, Indiana 47907

During replication, the lengthy genome of double-stranded DNA viruses is translocated with remarkable velocity into a limited space within the procapsid. The question of how this fascinating task is accomplished has long been a puzzle. Our recent investigation suggests that phi29 DNA packaging is accomplished by a mechanism similar to the driving of a bolt with a hex nut and that six packaging RNAs (pRNAs) form a hexagonal complex to gear the DNA-translocating machine (Chen, C., and Guo, P. (1997) *J. Virol.* 71, 3864–3871; Zhang, F., Lemieux, S., Wu, X., St.-Arnaud, S., McMurray, C. T., Major, F., and Anderson, D. (1998) *Mol. Cell* 2, 141–147; Guo, P., Zhang, C., Chen, C., Garver, K., and Trottier, M., (1998) *Mol. Cell* 2, 149–155). In the current study, circularly permuted pRNAs were used to position an azidophenacyl photoreactive cross-linking agent specifically at a strategic site that was predicted to be involved in pRNA-pRNA interaction. Cross-linked pRNA dimers were isolated, and the sites of cross-link were mapped by primer extension. The cross-linked pRNA dimer retained full activity in phi29 procapsid binding and genomic DNA translocation, indicating that the cross-link distance constraints identified in dimer formation reflect the native pRNA complex. Both cross-linked dimers either containing or not containing the interlocking loops for programmed hexamer formation bound procapsid equally well; however, only the one containing the interlocking loops programmed for hexamer formation was active in phi29 DNA packaging. The cross-linked pRNA dimers were also identified as the minimum binding unit necessary for procapsid binding. Primer extension of the purified cross-linked pRNA dimers revealed that base G^{82} was cross-linked to bases G^{39}, G^{40}, A^{41}, C^{49}, G^{62}, C^{63}, and C^{64}, which contribute to the formation of the three-way junction, suggesting that these bases are proximate in the formation of pRNA tertiary structure. Interestingly, the photoaffinity agent in the left interacting loop did not cross-link directly to the right loop as expected but cross-linked to bases adjacent to the right loop. These data provide a background for future modeling of pRNA tertiary structure.

The packaging RNA (pRNA)[1] of bacteriophage phi29 is a 120-base viral-encoded RNA molecule that is absolutely required in the packaging of viral DNA into its protein shell (1, 2). It has been shown that Mg^{2+} induces a conformational change of the pRNA (3), resulting in the binding of pRNA to the connector, the site where genomic DNA enters and exits the procapsid. The pRNA-enriched procapsids are competent to package DNA *in vitro* with the aid of a viral-encoded ATPase (gp16) and ATP (4). Upon completion of DNA packaging, the pRNA is released from the connector (5), and DNA-filled procapsid can subsequently be converted into infectious viral particles with the addition of neck and tail proteins (6, 7).

The connector of procapsids exhibits a 6-fold symmetry (8–15) and is embedded in a protein shell with a 5-fold rotational symmetry (16, 17). The relative motion of two rings could provide a driving force for DNA translocation (17). Recent studies have indicated an intermolecular interaction of pRNA through base pairing between the R loop (base 45–48) and L loop (bases 85–82) (Fig. 1) to form a pRNA hexameric complex to gear the viral DNA translocation machine (18, 19) (see Ref. 20 for minireview). Analogous to a car engine, sequential action of cylinders is a way to turn the motor. The finding that a hexameric pRNA complex bound to the connector and six pRNAs, worked sequentially (5), supports the proposal that the phi29 contains a rotary DNA-packaging machine (Fig. 2). Intensive investigation into pRNA structure and function has revealed that the pRNA contains two functional domains. One of them is the procapsid binding domain located in the middle of the sequence (21–24). The other is a domain composed of the proximal 5′- and 3′-end that is essential for DNA packaging but dispensable for procapsid binding (25, 26). It has been proposed that one domain of the pRNA binds to the connector, leaving the 5′/3′ domain free to interact with other components (21). It has also been proposed that pRNA possesses at least two conformations, a relaxed form and a contracted form. Alternating between contraction and relaxation of each member of the hexameric RNA complex driven by ATP hydrolysis may rotate the DNA translocation machine (Fig. 2) (5).

Understanding the specific role that the hexameric pRNA complex plays in viral DNA packaging requires structural knowledge of the pRNA. The pRNA secondary structure has been proposed through phylogenetic analysis (27, 28) and partially confirmed by nuclease probing (29), mutational analysis (25, 29–31), and cross-linking with psoralen (3) and bisphen (32). Compensatory modification has confirmed specific regions of the pRNA secondary structure, including the 5′/3′ proximal domain (25, 30) and the stem adjacent to the L loop (29). However, compensatory modification analysis on the secondary structure of the three-way junction adjacent to the R loop has generated contradictory results. Compensatory changing of the predicted base pairs $G^{38}G^{39}/C^{62}C^{63}$ to $A^{38}A^{39}/U^{62}U^{63}$ resulted in an pRNA that was not competent to compete with wild type pRNA for procapsid binding and retained only 50% DNA packaging activity (33, 34). Compensatory changing of the predicted base pairs 5′-$C^{50}U^{51}G^{52}A^{53}$/3′-$G^{61}A^{60}C^{59}U^{58}$ to 5′-

* This work was supported by National Science Foundation Grant MCB-9723923 and National Institutes of Health Grants GM48159 and GM59944 (to P. G.). The costs of publication of this article were defrayed in part by the payment of page charges. This article must therefore be hereby marked "*advertisement*" in accordance with 18 U.S.C. Section 1734 solely to indicate this fact.

‡ To whom correspondence should be addressed: Purdue Cancer Center, B-36 Hansen Life Science Research Bldg., Purdue University, West Lafayette, IN 47907. Tel.: 765-494-7561; Fax: 765-496-1795; E-mail: guo@vet.purdue.edu.

[1] The abbreviations used are: pRNA, packaging RNA; cp-pRNA, circularly permuted pRNA; GMPS, guanosine 5′-phosphorothioate; pfu, plaque-forming units; APA, azidophenacyl.

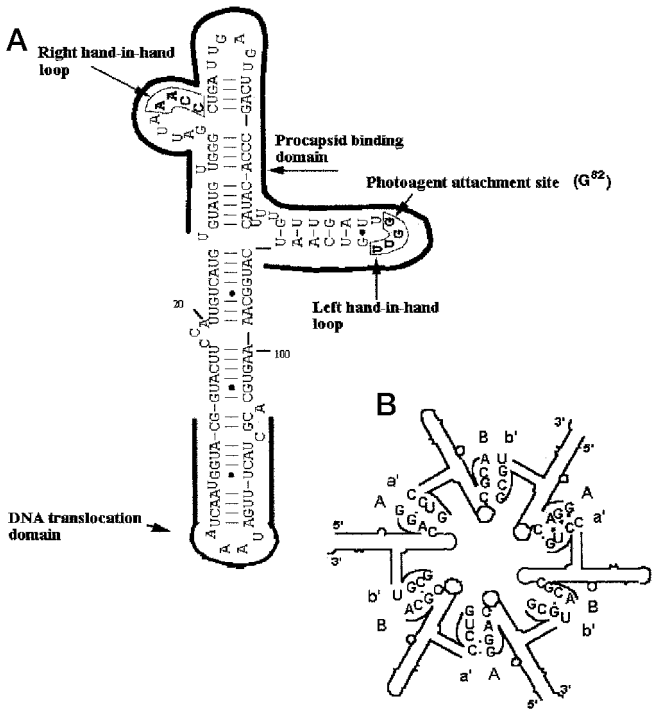

FIG. 1. *A*, sequence and predicted secondary structure of phi29 pRNA. The location of the photoagent attachment site is indicated with a *solid arrow*. The *numbers* indicate the base sequence of the native pRNA. The procapsid binding domain and the DNA translocation domain are marked with *bold lines*, and the four bases in the R and L loops responsible for inter-RNA interactions are *boxed* and in *bold*. *B*, diagram depicting the formation of a pRNA hexameric ring consisting of cp-pRNA B-a′ and pRNA A-b′ via the R and L hand-in-hand loop interaction.

$A^{50}G^{51}U^{52}C^{53}$/3′-$U^{61}C^{60}A^{59}G^{58}$ resulted in a pRNA that was neither competent for procapsid binding nor active in DNA packaging (34).

In this report, we used photoaffinity cross-linking to obtain information on the tertiary structure of RNA and to establish proximal regions between pRNA molecules. We used circularly permuted pRNAs (cp-pRNAs) (35–37) to attach a photosensitive cross-linking agent to a nucleotide predicted to be involved in forming a pRNA·pRNA complex in order to investigate its global architecture. We found that the cross-linked dimer retained full biological activity, indicating that the cross-links are relevant to the native structure of the pRNA complex. Primer extension of the intermolecular cross-links revealed several long range interactions that may contribute to the formation of pRNA·pRNA complexes. The bases, predicted within the secondary structure to form the three-way junction adjacent to the R loop, were confirmed to be proximate in the formation of the pRNA tertiary structure.

EXPERIMENTAL PROCEDURES

Preparation of pRNAs—cp-pRNAs were generated essentially as described in Zhang *et al.* (35). The primers used to produce DNA templates for cp-pRNA I-a′ and cp-pRNA B-a′ were: T7RNA82a′, 5′-TAATACGACTCACTATAGTCCGTCAATCATGGCA-3′; 3′RNA81I, 5′-AATCAACAAAGTATGTG-3′; 3′RNA81B, 5′-AATCAACAAAGTATGTGGGCTGAACTCAATCAGGCGTTAATC-3′.

To produce pRNA A-b′, template DNA was produced by polymerase chain reaction using *Taq* DNA polymerase (Promega) and two overlapping oligonucleotide primers. These primers were: 5′T7A: 5′-TAATACGACTCACTATAGGAATGGTACGGTACTTCCATTGTCATGATTAGGACCT GATTGAGTTCAGCCCAC-3′. 3′Pb′: 5′-CTTAAGGAAAGTAGCGTGCACTTTTGCCATGATTGACACGCAATCAACAAAGTATGTGGGCTGAACTCAATC-3′.

The polymerase chain reaction fragment that contained 3′-A overhangs due to the inherent activity of *Taq* was subcloned into the pGEM plasmid (Promega) containing 5′-T overhangs. The plasmid was then sequenced. Template DNA utilized in *in vitro* transcription was generated by cutting the pGEM plasmid with restriction enzymes *Nco*I and *Nde*I.

The resulting DNA templates were utilized in *in vitro* transcription containing T7 RNA polymerase (21). Transcripts were purified by electrophoresis through 8% polyacrylamide, 8 M urea gels, viewed by UV shadow, and passively eluted into 0.5 M ammonium acetate, 0.1% SDS, and 0.1 mM EDTA.

Preparation of Photoagent-containing cp-pRNAs—GMPS-containing cp-pRNAs were prepared by *in vitro* transcription of DNA templates with T7 RNA polymerase in the presence of 40 mM Tris-HCl, pH 7.5, 12 mM $MgCl_2$, 2 mM spermidine, 10 mM NaCl, 1 mM ATP, 1 mM CTP, 1 mM UTP, 0.2 mM GTP, [α-^{32}P]GTP, 8 mM GMPS (Amersham Pharmacia Biotech) at 37 °C for 4 h. Transcripts were purified by electrophoresis through 8% polyacrylamide, 8 M urea gels, viewed by autoradiography, and passively eluted into 10 mM Tris-HCl, pH 8, 0.3 M sodium acetate, 1 mM EDTA, and 0.1% SDS. Transcripts were ethanol-precipitated and dried vacuum-dried. Transcripts containing the 5′-terminal phosphate of 5′-guanosine monophosphorothioate were coupled to an azidophenacyl group (38).

Cross-linking—The formation of pRNA·pRNA complexes were achieved by mixing equal molar amounts of 75 nM photoagent-containing cp-pRNA, such as N_3-cp-[^{32}P]pRNA I-a′ and a transcomplementary pRNA in TMS (50 mM Tris-HCl, pH 7.8, 10 mM $MgCl_2$, 100 mM NaCl). The pRNAs were incubated on ice for 15 min and then exposed to UV light (Phillips, UVB 20 W-TL01, 311 nm) for 15–30 min at 0 °C. Under these conditions, no photoagent-independent cross-links were detected. The efficiency of intra- and inter-molecular cross-links (Table II) were measured as a fraction of the total input azido-pRNA using densitometric readings of individual intra- and inter-molecular-cross-linked bands.

Primer Extension Analysis—Intermolecular cp-pRNA/pRNA-cross-linked conjugates were resolved by electrophoresis through 10% polyacrylamide, 8 M urea, TBE (90 mM Tris-HCl, pH 8.0, 89 mM boric acid, 2 mM EDTA) gels. Intermolecular cross-links were identified by autoradiography and electroeluted in 20 mM Tris-HCl, pH 8, 5 mM NaCl, 1 mM EDTA at 120 V for 15 min. The amount of cp-pRNA in each intermolecular cross-link sample was determined by the comparison of radioactive counts between a known amount of cp-pRNA used for cross-linking and that of the cp-pRNA·pRNA complex after purification. 5′ ^{32}P-labeled oligonucleotide primer specific for pRNA A-b′ was hybridized to varying amounts of purified intermolecular cross-link species (75 °C for 2 min, then slowly cooled over 10 min to 37 °C). The primer sequence was: 5′-GCCGCGGGATTCTTAAGGAAAGTA-3′. Oligonucleotides were extended by AMV reverse transcriptase at 45 °C for 20 min. The products were resolved by electrophoresis through 8% polyacrylamide, 8 M urea, TBE gels.

DNA Packaging Activity Assayed by in Vitro Phi29 Assembly—The purification of the DNA packaging enzyme gp16 (39), DNA-gp3 (6), procapsid (40, 41), and the preparation of other accessory proteins, gp9 (42), gp11, gp12, and gp13 (6), has been described previously.

To reconstitute procapsids with pRNA, 10–100 ng of pRNA (10^{11-12} molecules) was mixed with 2.4×10^{11} procapsids (20 ng) and dialyzed against TBE buffer (89 mM Tris-HCl, pH 8.3, 89 mM boric acid, 2.5 mM EDTA) for 15 min on a 0.025-μm membrane filter (type VS, Millipore Corp.) at ambient temperature, then against TMS buffer for an additional 30 min. Procapsids (4 mg/ml) were quantified by measuring the absorbance at 280 nm (A_{280}) or by SDS-polyacrylamide gel electrophoresis with reference to protein standards. The biological activity of the procapsid assembled in *Escherichia coli* was tested in the defined DNA packaging system (39, 43). The phi29 DNA·gp3 (0.1 mg/ml) complex was dialyzed against TMS buffer for 40 min on a 0.025-mm membrane filter at ambient temperature, and the DNA packaging protein gp16 (0.5 mg/ml) was dialyzed against 10 mM Tris-HCl, pH 7.8, 4 mM KCl for 40 min on ice. After dialysis, the procapsids were mixed with phi29 DNA-gp3, gp16, and reaction buffer (10 mM ATP, 6 mM spermidine, 3 mM β-mercaptoethanol, 50 mM Tris-HCl, pH 7.8, 10 mM $MgCl_2$, and 100 mM NaCl) with the volume ratio of 5:3.5:1.5:1.5 and incubated for 30 min at room temperature. The DNA-filled capsids were converted into infectious virions *in vitro* with the addition of tail protein (gp9), neck proteins (gp11 and gp12), and morphogenic factor (gp13), which were also produced from cloned genes. Typically, 10^7 plaque-forming units (pfu)/ml were obtained with wild type pRNA, and omission of any one of the component resulted in no plaque formation. The *in vitro* assembly of infectious virus from synthetic components provided a highly sensitive system for the assay of pRNA function. The sensitivity of this system is such that the generation of a single infectious virion could be detected due to the absence of any background.

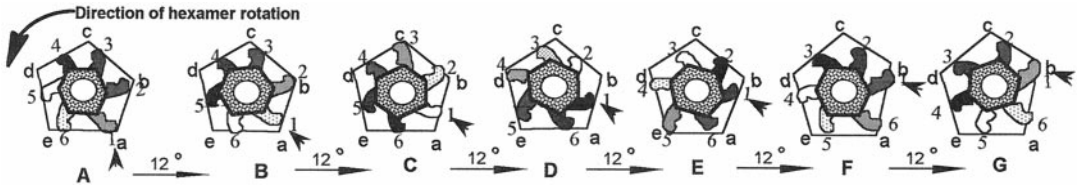

FIG. 2. **A model (from Ref. 5) depicting sequential action of pRNA to gear the DNA translocation machine.** The *hexagons* and surrounding *pentagons* symbolize the connector and capsid membrane, respectively. Six protrusions symbolize six pRNAs. The *arrows* point to the different energetic states of pRNA 1 with variable patterns to illustrate different energetic conformation. A to G depicts 6 steps of a 12° rotation (a 5/6-fold mismatch generates 30 equivalent orientations, 360° ÷ 30 = 12°). Each pRNA rotates 72° after 6 steps to move from one vertex to an adjacent vertex (pRNA 1 moves from vertex a to b). If 1 ATP is needed for 1 pRNA to move from one vertex to another via 1 cycle of contraction and relaxation, then 30 ATPs (6 RNA × 5 vertices) are needed for a 360^0 rotation that cause the translocation of one helical turn or 10.5 bases of DNA.

TABLE I
Procapsid binding and DNA packaging activities of pRNA species

pRNA species	Right | | | | loop sequence Left	Procapsid binding efficiency[1] (%)	DNA packaging activity (PFU/ml)	Predicted hexamer[2]
I-i' (wild type pRNA alone)	I 5'-AACC-3' | | | | i 3'-UUGG-5'	53	5.0×10^7	Active
I-a' 82/81 (unpaired loops)	I 5'-AACC-3' | a' 3'-CCUG-5'	6.7	0	Inactive
B-a' 82/81 (unpaired loops)	B 5'-ACGC-3' | a' 3'-CCUG-5'	3.6	0	Inactive
A-b' (unpaired loops)	A 5'-GGAC-3' | b' 3'-UGCG-5'	7.7	0	Inactive
(I-a') + (A-b') (unpaired loop)	I 5'-AACC-3' | b' 3'-UGCG-5' A 5'-GGAC-3' | | | | a' 3'-CCUG-5'	20	0	Inactive
(B-a') + (A-b') (compensatory pair)	B 5'-ACGC-3' | | | | b' 3'-UGCG-5' A 5'GGAC-3' | | | | a' 3'-CCUG-5'	52	5.2×10^7	Active

[1] Binding efficiency is expressed as a percentage of the total input pRNA bound to purified procapsids.
[2] Diagram showing the interaction of pRNA right and left loops in the formation of a hexameric complex. The uppercase letters stand for the right loop, and the lowercase letters stand for the left loop. The same letter in upper- and lowercase represents two sequences that are complementary. The "‖" at the vertices indicates that the two loops are noncomplementary.

The activity of each RNA reported in this paper was measured by the number of pfu/ml produced when the pRNAs were used in the viral assembly assay (30), since it is well documented that the pRNA only participates in the step of DNA packaging (1, 5, 40). No experimental attempt was made to distinguish the activity for phi29 virion assembly and DNA packaging. The activity is based solely on the number of plaques produced. pRNA molecules that produced fewer pfu/ml than the wild type control pRNA when used in the plaque-forming assay were said to have reduced activity.

Procapsid-pRNA Binding Assays—Sucrose gradient sedimentation of procapsid-[^{32}P]pRNA was performed to detect the presence of procapsid-pRNA complexes (2). Briefly, pRNA (60 ng, 10^{12} molecules) was mixed with 10 μl of purified procapsid (4 mg/ml, 10^{12} molecules) and dialyzed as above against TBE buffer for 15 min at ambient temperature. The mixtures were then dialyzed against TMS buffer for 30 min at ambient temperature. After the incubation, the mixtures were diluted to 0.1 ml in TMS and loaded onto the top of a 5–20% sucrose gradient in TMS and spun in a Beckman L-80 Ultracentrifuge at 35,000 rpm for 30 min at 20 °C in an SW 55 rotor. After centrifugation, fractions were collected from the bottom of the tube and prepared for scintillation counting. The value for each gradient fraction was plotted as a percentage of the total radioactivity recovered from that gradient.

RESULTS

Structural Relevance of cp-pRNAs Used in Cross-linking Analysis—Site-specific photoagent attachment sites located in the interior of the pRNA were made possible with the use of cp-pRNA (35). In this study, mutant cp-pRNAs were constructed such that the attachment of a photoagent at the new 5′ termini would provide information bearing on regions of the structure involved in inter-pRNA interaction. Recent studies

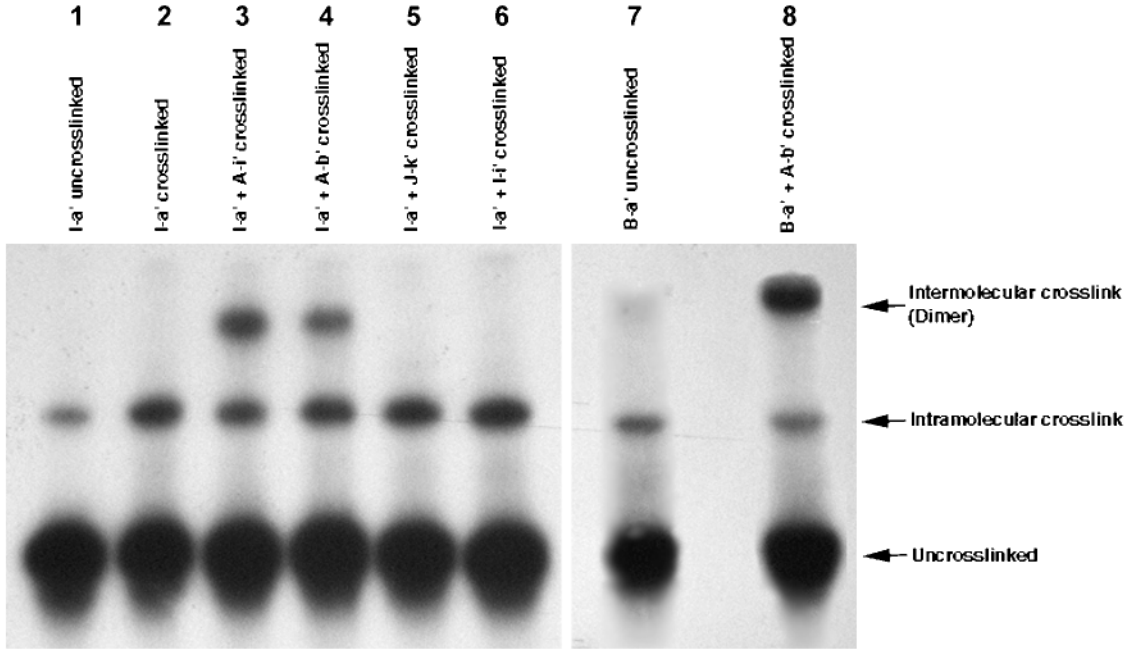

FIG. 3. **Separation of cross-linked and uncross-linked pRNA in denaturing acrylamide gels.** N_3-cp-[^{32}P]pRNA I-a′ and N_3-cp-[^{32}P]pRNA B-a′ alone or mixed with other unlabeled mutant pRNAs were cross-linked with UV (*lanes 2–6* and *8*). The *lane* marked uncross-linked was not exposed to 311-nm UV light, although due to exposure to ambient light, some intramolecular cross-links were observed (*lanes 1* and *7*). This figure is a composite, both B-a′-uncross-linked and B-a′ + A-b′-cross-linked samples (*lanes 7* and *8*) were run on a separate gel therefore exhibiting slightly different mobilities

TABLE II
Analysis of cross-linked species

NA, not applicable.

Cross-linked species	Efficiency of cross-linked[a]	Procapsid binding efficiency[b]	DNA packaging activity	Cross-linked nucleotide
	%	%	*pfu/ml*	
I-i′ (wild type pRNA)	NA	51.2	1.9×10^6	NA
[5′-N_3]I-a′	17.3	2.4	0	NA
[5′-N_3]B-a′	14.2	4.7	0	NA
[5′-N_3]I-a′/A-b′	19.1	64.8	0	G^{39},G^{40},A^{41},C^{49},G^{62},C^{63},C^{64}
[5′-N_3]B-a′/A-b′	31.5	61.9	2.2×10^6	G^{39},G^{40},A^{41},C^{49},G^{62},C^{63},C^{64}

[a] Efficiency of cross-link indicates percent conversion to cross-linked species.
[b] Procapsid binding efficiency is expressed as a percentage of the total input pRNA bound to purified procapsids as assayed by sucrose gradient sedimentation.

have shown an intermolecular interaction of pRNA through base pairing between the R loop (base 45–48) and the L loop (base 85–82) (Fig. 1) (18–20). Therefore mutant cp-pRNAs repositioning the 5′ and 3′ termini to bases 82 and 81, respectively, were developed such that a photoagent can be attached at a base involved in the interaction.

As with all circularly permuted RNA constructs, the location of the new end points may disrupt the native structure and therefore may not be structurally relevant. To ensure that the cp-pRNAs used in the present analysis maintained a native conformation, the cp-pRNAs were tested for their participation in procapsid binding and DNA packaging. Cp-pRNAs and pRNAs were constructed with alteration in the R and L loops (Table I). The uppercase and lowercase letters are used to represent the R and L loop sequences, respectively. The same letter in upper- and lowercase represents a pair of complementary sequences, whereas different letters indicate noncomplementary loop sequences. For example, in cp-pRNA I-I′ (wild type sequence), the R loop sequence I (5′-$A^{45}A^{46}C^{47}C^{48}$-3′) and L loop sequence i′ (3′-$U^{85}U^{84}G^{83}G^{82}$-5′) are complementary, whereas in cp-pRNA I-a′, the R loop sequence I is not complementary to the L loop sequence a′ (3′-$C^{85}C^{84}U^{83}G^{82}$-5′). All pRNAs that had mutations resulting in unpaired R and L loops, such as cp-pRNAs I-a′, B-a′, and pRNA A-b′, when used individually, showed an inability to interact intermolecularly and a reduced binding to prohead and were inactive in DNA packaging as assayed by *in vitro* phi29 assembly (Table I). However, when two inactive pRNAs that were transcomplementary in their R and L loops, for example cp-pRNA B-a′ and pRNA A-b′, were mixed in a 1:1 molar ratio, an intermolecular interaction was observed, procapsid binding was as efficient as wild type, and full packaging activity was restored (Table I).

Mutants cp-pRNA I-a′ and pRNA A-b′ were constructed to allow us to compare an inactive oligomeric pRNA complex to an active pRNA complex. When incubated together these pRNAs have the ability to form an open dimer but are unable to form higher multimers. The resulting pRNA complex was able to bind procapsids, although it was inactive in DNA packaging (Table I). These RNAs represented a functionally inactive pRNA complex.

Distinction between Intra- and Inter-RNA Cross-links Using Circularly Permuted pRNAs—To cross-link cp-pRNAs, an azidophenacyl (APA) group was attached to the 5′-end of individual cp-pRNAs. For 5′-modification, the APA group was attached to cp-pRNAs containing a GMPS incorporated at base 82 during transcription. GMPS was modified with photoreactive azidophenacyl bromide (44, 45). The photoaffinity-modified cp-pRNAs were then irradiated with 311-nm light, which con-

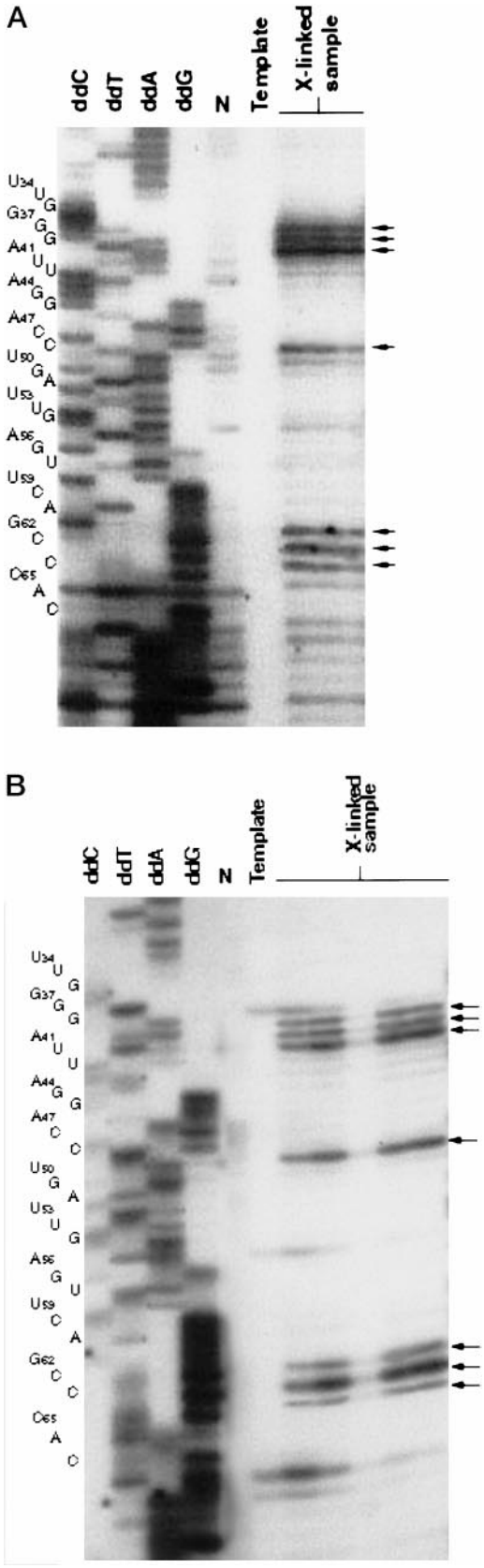

FIG. 4. **Primer extension to map the sites of intermolecular cross-linking between N_3-cp-[^{32}P]pRNA I-a′ and pRNA A-b′ (*A*) as well as N_3-cp-[^{32}P]pRNA B-a′ and pRNA A-b′ (*B*).** The G, A, T, and C denote *lanes* containing G, A, T, C sequencing reactions; *N* is a control primer extension from noncross-linked pRNA A-b′. The *lanes* marked *Template* in both *A* and *B* contain only N_3-cp-[^{32}P]pRNA I-a′ and N_3-cp-[^{32}P]pRNA B-a′, respectively. The *lanes* contained within the region marked *X-link sample* represent multiple primer extension reactions containing various concentrations of gel-purified intermolecular-cross-linked pRNA template. A primer specific to pRNA A-b′ was used for extension.

verts the azido group to a highly reactive nitrene, which is able to insert into a variety of covalent bonds. An APA derivative was used to provide long range cross-links with which we hoped to identify general features of the RNA-RNA interaction.

To characterize the cross-linking reactions, UV-treated photoagent-modified cp-pRNAs were resolved on denaturing polyacrylamide gels. The cross-linked species appeared as bands migrating more slowly than uncross-linked RNA (Fig. 3). Cross-linking of APA-modified cp-pRNAs occurred exclusively via the azidophenacyl moiety, because unconjugated RNA did not form cross-links, and the photoagent treated with phenyl mercuric acetate eliminated the slower migrating bands (data not shown). The conversion of the analyzed pRNAs containing the photoagent into cross-linked species was efficient, between 10 and 30% (Table II). Fig. 3 shows the cross-linking results obtained with two 5′-APA cp-pRNAs alone and in the presence of a transcomplementary pRNA. Intramolecular cross-links appeared in each of the cross-linking reactions. The formation of these intramolecular cross-links were differentiated between intra- and inter-RNA cross-links by assessing the sensitivity of the cross-linking reaction to dilution. Dilution up to 100-fold of cross-linking reactions containing 5′-APA cp-pRNAs alone and in the presence of a transcomplementary pRNA did not affect the efficiency in the formation of the band representing the intra-pRNA cross-links, whereas the efficiency in the formation of the band representing the inter-pRNA cross-link was significantly reduced (data not shown).

Intermolecular cross-linking was accomplished by the pairing of the R loop of pRNA A-b′ with the L loop of either cp-pRNA I-a′ or B-a′ (Fig. 3). The L loop (a′) contained the photoreactive group and was able to interact with the complementary R loop (A) in the other pRNA. This dimeric complex is specific to the interaction of transcomplementary loop(s). When two mutant pRNAs without transcomplementary loop(s) were incubated and cross-linked, no intermolecular cross-links were observed (Fig. 3).

Analysis of Inter-RNA Cross-linking Sites—The particular nucleotides cross-linked to the modified termini of the cp-pRNA were determined by primer extension (Fig. 4). Individual intermolecular-cross-linked species were gel-purified and used as templates for primer extension with reverse transcriptase. Reverse transcriptase terminates one nucleotide 3′ to cross-link sites in the RNA template (46–49). The analysis for the intermolecular-cross-linked species derived from I-a′/A-b′ and B-a′/A-b′ are shown in Fig. 4*B*. Intermolecular cross-links were mapped by primer extension using a primer specific to the 3′ end of pRNA A-b′. Comparison of extension products from noncross-linked RNA and sequencing reactions identified the individual cross-linked nucleotides (Table II). The location of the cross-linked sites for the two intermolecular-cross-linked conjugates (I-a′/A-b′ and B-a′/A-b′) were found to be identical and mapped to nucleotides G^{39}, G^{40}, A^{41}, C^{49}, G^{62}, C^{63}, C^{64}, suggesting that these bases are proximate in the formation of pRNA tertiary structure.

Intramolecular cross-link species were not analyzed in this study because they were inactive in viral DNA packaging. Thus, the biologically nonfunctional intramolecular-cross-linked species were not considered as structurally relevant models to be investigated further.

Procapsid Binding and DNA Packaging Activity of Intermolecular-cross-linked Species—To assess the relevance of the cross-linking and gain insight into the mechanism by which

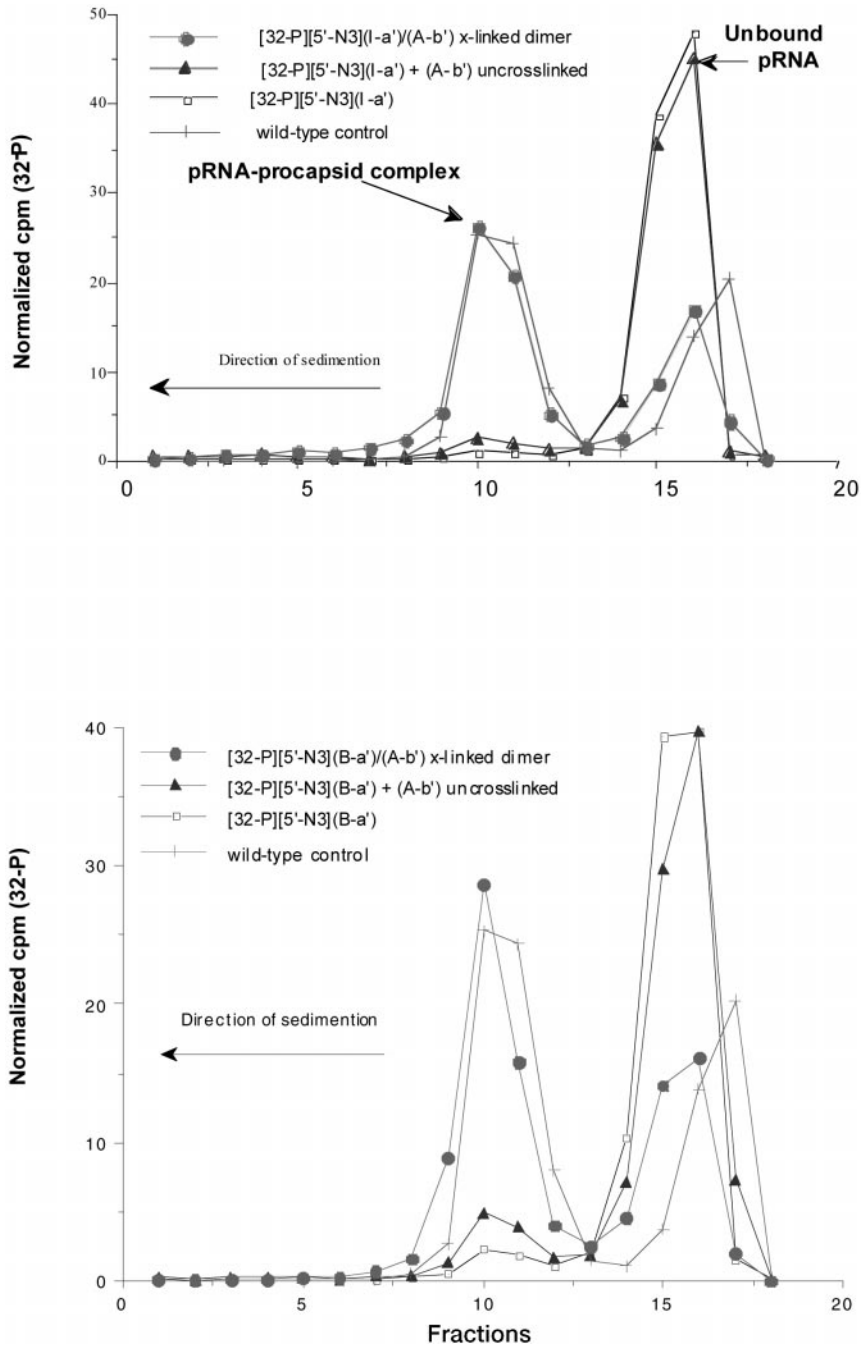

FIG. 5. **Sucrose gradient sedimentation to analyze the binding of pRNA to procapsid.** Purified procapsids were mixed with pRNA samples and sedimented in an ultracentrifuge. Free monomeric pRNA remained near the top of the gradient, whereas the dimeric pRNA complexes bound to procapsids and co-sedimented into the gradient and center at fraction 10.

pRNA functions, further comparison of the individual gel-purified cross-linked species for their ability to bind procapsids and package DNA was performed. To test for the ability of cross-linked RNA to bind procapsids, intermolecular-cross-linked species were gel-purified and incubated with purified procapsids in the presence of Mg^{2+}. Control reactions containing noncross-linked RNA incubated with purified procapsids and Mg^{2+} were also performed. The pRNA-enriched procapsid complexes were sedimented through sucrose gradients, and fractions were collected (Fig. 5). The gel-purified intermolecular cross-link species, both I-a′/A-b′ and B-a′/A-b′, retained substantial procapsid binding activity.

To analyze the DNA packaging activity, intermolecular cross-links were gel-purified and utilized in *in vitro* phi29 assembly. Under identical conditions to those used in assessing the DNA packaging activity of uncross-linked cp-pRNAs, intermolecular cross-links showed similar activity with respect to their uncross-linked counterparts. Intermolecular cross-link conjugate cp-pRNA B-a′/A-b′, of which the two pairs of interacting loops allow for the formation of a cyclic hexamer, retained DNA packaging activity, whereas intermolecular cross-link conjugate cp-pRNA I-a′/A-b′, of which the two pairs of interacting loops only allow for the formation of a open dimer, was inactive in DNA packaging. Thus, the substantial retention and lack of biological activities exhibited by the intermolecular-cross-linked species B-a′/A-b′ and I-a′/A-b′, respectively, lends relevance of the cross-linking data to the native (active) conformation of the pRNA.

DISCUSSION

These experiments provide the first structural constraints that bear on the oligomeric pRNA complex. Using circularly permuted pRNAs containing a photoagent attached to a phosphate on which a transcomplementary pRNA loop interacts

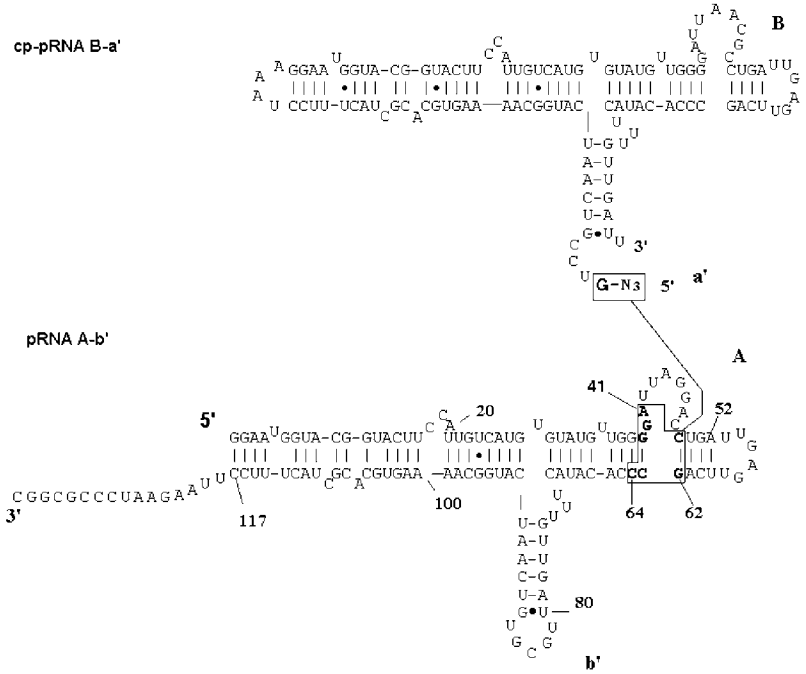

FIG. 6. **Summary of pRNA intermolecular cross-linking sites marked with polygons.** Diagram depicts the use of cp-pRNA B-a′ for photoagent attachment to cross-link to pRNA A-b′, although identical intermolecular cross-link sites are detected using cp-pRNA I-a′.

allowed intermolecular pRNA cross-links to be isolated. Interestingly, the photoaffinity agent in the left interacting loop did not cross-link directly to the right loop as expected but cross-linked to bases adjacent to the right loop. The cross-linking observed is both highly efficient (10–30%) and specific, occurring at only a few nucleotides in each of the transcomplementary pRNAs. Moreover, transcomplementary pRNA B-a′/A-b′ that exhibited both full procapsid binding and DNA packaging activity retained such activity when existing as a cross-linked conjugate. Thus, the data indicate that the cross-linked inter-pRNA conjugates mimic those interactions involved in the formation of hexameric pRNA complexes.

The high efficiency of cross-linking observed lends credibility to the structural relevance of the cross-linked species formed. Presumably, the cross-linked species obtained with high efficiency most likely, but not conclusively, represent the most stable (native) structure in the population. Thus pRNAs that adopt the most active (native) conformation yield the most efficient cross-link. The higher efficiency of intermolecular cross-linking that we observed in the reactions containing pRNA pair B-a′/A-b′ is probably due to the fact that in this pair both R and L loops are transcomplementary, although in the inactive pRNA pair I-a′/(A-b′ only the L loop a′ of pRNA I-a′ is transcomplementary to the R loop A of pRNA A-b′.

It is noteworthy that individual inter-pRNA-cross-linked conjugates maintained their ability to perform specific biological functions. This again adds to the validity that the cross-linking results obtained in this study may be taken as meaningful constraints on the structure of oligomeric pRNA complexes. The active pRNA pair B-a′/A-b′ allows not only for the formation of dimers but also higher multimers, as demonstrated by its competency to package phi29 DNA into procapsid, a process that requires the formation of a pRNA hexamer (18, 20). Mutant pair I-a′/A-b′ can transcomplement to form dimers but cannot package phi29 DNA, whereas both intermolecular pRNA cross-link conjugates B-a′/A-b′ and I-a′/A-b′ possess similar procapsid binding efficiencies. Therefore, the dimeric pRNA complex is sufficient to achieve full procapsid binding. Further support for this is indicated by the reduced binding efficiency of an uncross-linked mixture of pRNA I-a′ and A-b′. These pRNAs, due to a reduced ability to form dimers (as discussed above), when incubated together consist of both pRNA monomers and dimers. Consequently, pRNA monomers are unable to bind procapsid (Table I and II and Fig. 5), and therefore the mixture possesses a reduced efficiency in procapsid binding as compared with its purified intermolecular cross-link counterpart. Hence pRNA dimers represent the minimum binding unit necessary for procapsid binding.

It is interesting to note that the cross-linked sites of both the biologically inactive and active intermolecular-cross-linked conjugates are identical. The photoagent-modified pRNAs vary from one another in the sequence of the R loop but contain common secondary structures. Presumably, the photoagent-modified R loop sequence of the pRNA and interaction with its transcomplementary L loop did not affect the structural features of the L loop with its transcomplementary loop. Based on this result and the secondary structure (Fig. 1), it can be easily imagined that the R and L loops are distant from one another and possibly separated in the tertiary structure such that each loop can interact individually with its transcomplementary loop. The secondary structure positions the cross-link sites to those nucleotides surrounding the base of the R loop (Fig. 6). Previous mutational studies using pRNAs with deleted bases within the R loop area (specifically bases G^{38} and G^{39}) resulted in a pRNA that is inactive in both procapsid binding and DNA packaging (31). These data further support our finding that the cross-link sites identified in this study may be involved in an inter-pRNA interaction.

Comparison of the active intermolecular-cross-linked pRNA dimer B-a′/A-b′ to that of the inactive intermolecular-cross-linked pRNA dimer I-a′/A-b′ indicated that both intermolecular complexes have structural and procapsid binding similarities. Although these similarities exist between the two pRNA complexes, they differ dramatically in their ability to package DNA. The pRNA complex B-a′/A-b′ maintained the ability to form not only a dimer but also an interlocking hexameric ring, which is needed for DNA translocation (18). Conversely, the pRNA complex I-a′/A-b′, which is able to form dimers, might not be able to form an interlocking hexameric ring. Thus, the results presented here support previously reported data indicating that an interlocking hexameric pRNA complex is essential for DNA packaging.

Finally, we note that the results reported here place constraints on structure models. With an expanded body of cross-linking results and available data concerning pRNA secondary structure, we will be able to develop a model of the structure of the pRNA hexameric complex.

Acknowledgments—We thank Dr. Harry Morrison and Dr. Taj Mohammed for the use of the 311-nm light source. We also thank Dr. Norman Pace, James Nolan, and Michael Harris for their valuable advice and comments on the use of the site-directed photocross-linking method.

REFERENCES

1. Guo, P., Erickson, S., and Anderson, D. (1987) *Science* **236,** 690–694
2. Guo, P., Bailey, S., Bodley, J. W., and Anderson, D. (1987) *Nucleic Acids Res.* **15,** 7081–7090
3. Chen, C., and Guo, P. (1997) *J. Virol.* **71,** 495–500
4. Guo, P., Peterson, C., and Anderson, D. (1987) *J. Mol. Biol.* **197,** 229–236
5. Chen, C., and Guo, P. (1997) *J. Virol.* **71,** 3864–3871
6. Lee, C. S., and Guo, P. (1994) *Virology* **202,** 1039–1042
7. Lee, C. S., and Guo, P. (1995) *J. Virol.* **69,** 5018–5023
8. Herranz, L., Salas, M., and Carrascosa, J. L. (1986) *Virology* **155,** 289–292
9. Valpuesta, J. M., Fujisawa, H., Marco, S., Carazo, J. M., and Carrascosa, J. (1992) *J. Mol. Biol.* **224,** 103–112
10. Turnquist, S., Simon, M., Egelman, E., and Anderson, D. (1992) *Proc. Natl. Acad. Sci. U. S. A.* **89,** 10479–10483
11. Kochan, J., Carrascosa, J. L., and Murialdo, H. (1984) *J. Mol. Biol.* **174,** 433–447
12. Cerritelli, M. E., and Studier, F. W. (1996) *J. Mol. Biol.* **285,** 299–307
13. Yeo, A., and Feiss, M. (1995) *J. Mol. Biol.* **245,** 141–150
14. Rishovd, S., Holzenburg, A., Johansen, B. V., and Lindqvist, B. H. (1998) *Virology* **245,** 11–17
15. Guasch, A., Pous, J., Parraga, A., Valpuesta, J. M., Carrascosa, J. L., and Coll, M. (1998) *J. Mol. Biol.* **281,** 219–225
16. Caspar, D. L. D., and Klug, A. (1962) *Cold Spring Harbor Symp. Quant. Biol.* **27,** 1–24
17. Hendrix, R. W. (1978) *Proc. Natl. Acad. Sci. U. S. A.* **75,** 4779–4783
18. Guo, P., Zhang, C., Chen, C., Garver, K., and Trottier, M. (1998) *Mol. Cell* **2,** 149–155
19. Zhang, F., Lemieux, S., Wu, X., St.-Arnaud, S., McMurray, C. T., Major, F., and Anderson, D. (1998) *Mol. Cell* **2,** 141–147
20. Hendrix, R. W. (1998) *Cell* **94,** 147–150
21. Garver, K., and Guo, P. (1997) *RNA* (*N. Y.*) **3,** 1068–1079
22. Trottier, M., Zhang, C. L., and Guo, P. (1996) *J. Virol.* **70,** 55–61
23. Trottier, M., and Guo, P. (1997) *J. Virol.* **71,** 487–494
24. Reid, R. J. D., Bodley, J. W., and Anderson, D. (1994) *J. Biol. Chem.* **269,** 5157–5162
25. Zhang, C. L., Lee, C.-S., and Guo, P. (1994) *Virology* **201,** 77–85
26. Zhang, C. L., Garver, K., and Guo, P. (1995) *Virology* **211,** 568–576
27. Bailey, S., Wichitwechkarn, J., Johnson, D., Reilly, B., Anderson, D., and Bodley, J. W. (1990) *J. Biol. Chem.* **265,** 22365–22370
28. Chen, C., Zhang, C., and Guo, P. (1999) *RNA* (*N. Y.*) **5,** 805–818
29. Reid, R. J. D., Zhang, F., Benson, S., and Anderson, D. (1994) *J. Biol. Chem.* **269,** 18656–18661
30. Zhang, C. L., Tellinghuisen, T., and Guo, P. (1995) *RNA* (*N. Y.*) **1,** 1041–1050
31. Zhang, C. L., Tellinghuisen, T., and Guo, P. (1997) *RNA* (*N. Y.*) **3,** 315–322
32. Mohammad, T., Chen, C., Guo, P., and Morrison, H. (1999) *Bioorg. Med. Chem. Lett.* **9,** 1703–1708
33. Wichitwechkarn, J., Johnson, D., and Anderson, D. (1992) *J. Mol. Biol.* **223,** 991–998
34. Reid, R. J. D., Bodley, J. W., and Anderson, D. (1994) *J. Biol. Chem.* **269,** 9084–9089
35. Zhang, C. L., Trottier, M., and Guo, P. X. (1995) *Virology* **207,** 442–451
36. Nolan, J. M., Burke, D. H., and Pace, N. R. (1993) *Science* **261,** 762–765
37. Pan, T., Gutell, R. R., and Uhlenbeck, O. C. (1991) *Science* **254,** 1361–1364
38. Burgin, A. B., and Pace, N. R. (1990) *EMBO J.* **9,** 4111–4118
39. Guo, P., Grimes, S., and Anderson, D. (1986) *Proc. Natl. Acad. Sci. U. S. A.* **83,** 3505–3509
40. Guo, P., Rajogopal, B., Anderson, D., Erickson, S., and Lee, C.-S. (1991) *Virology* **185,** 395–400
41. Guo, P., Erickson, S., Xu, W., Olson, N., Baker, T. S., and Anderson, D. (1991) *Virology* **183,** 366–373
42. Lee, C. S., and Guo, P. (1995) *J. Virol.* **69,** 5024–5032
43. Grimes, S., and Anderson, D. (1989) *J. Mol. Biol.* **209,** 91–100
44. Hanna, M. M., and Meares, C. F. (1983) *Biochemistry* **22,** 3547–3551
45. Hixon, S. H., and Hixon, S. S. (1975) *Biochemistry* **14,** 4251–4254
46. Hagenbuchle, O., Santer, M., and Steitz, J. A. (1978) *Cell* **13,** 551–563
47. Youvan, D. C., and Hearst, J. E. (1982) *Anal. Biochem.* **119,** 86–89
48. Barta, A., Steiner, G., Brosinus, J., Noller, H. F., and Kuechler, E. (1984) *Proc. Natl. Acad. Sci. U. S. A.* **81,** 3607–3611
49. Inoue, T., and Cech, T. R. (1985) *Proc. Natl. Acad. Sci. U. S. A.* **82,** 648–652